Effect of walls on the supersonic reacting mixing layer

By D. S. Shin AND J. H. Ferziger[1]

1. Motivation and objectives

Most stability analyses of supersonic mixing layers have considered unconfined shear layers. However, the supersonic mixing layers in ramjet combustors and most experiments are confined by solid walls. Two distinct types of instabilities may occur in confined shear layers. One is the Kelvin-Helmholtz instability found in subsonic shear layers; the other is the acoustic instability. In low speed flows, the effects of walls on the Kelvin-Helmholtz instability are relatively small so long as they are separated by many shear layer thicknesses. However, in high speed flows, some of the energy of the acoustic radiation that would leave an infinite system is reflected from the walls. This reflection can alter the stability characteristics of the flow significantly (Tam and Hu 1989; Greenough *et al.* 1989; Zhuang *et al.* 1990; Morris and Giridharan 1991).

To include the effect of chemical reaction, we shall consider a reacting mixing layer in a channel. The chemistry model is finite rate single step irreversible reaction with Arrhenius kinetics. Laminar flows obtained by solving the compressible boundary-layer equations (Shin and Ferziger 1991) are used as the basis for the stability study because the confining walls hardly change the profiles of laminar flows (see Fig. 1). All flow variables are nondimensionalized by their fast-stream values.

We shall consider the effects of heat release, Mach number, frequency, wavenumber, thickness of shear layer, as well as distance between walls and direction of propagation of the disturbance waves. We use non-dimensional adiabatic flame temperature, T_{ad}, to express the amount of heat release from combustion. Note that for a given T_{ad}, the actual temperature rise in high Mach number flows may be higher than that of low Mach number flows because of viscous dissipation. How best to express the temperature rise from the combustion and viscous dissipation in a single parameter is still an open question.

2. Accomplishments

2.1 Inviscid linear stability equation

We consider a spatially developing plane mixing layer in which the fuel and oxidizer are initially unmixed. The flow is confined to a rectangular channel of height $2H$ and breadth B. We assume locally parallel mean flow and small wavelike disturbances propagating in x direction. Each dimensionless quantity can be expressed as

$$F(x,y,z,t) = \overline{F}(y) + F'(x,y,z,t) \tag{1}$$

1 Stanford University.

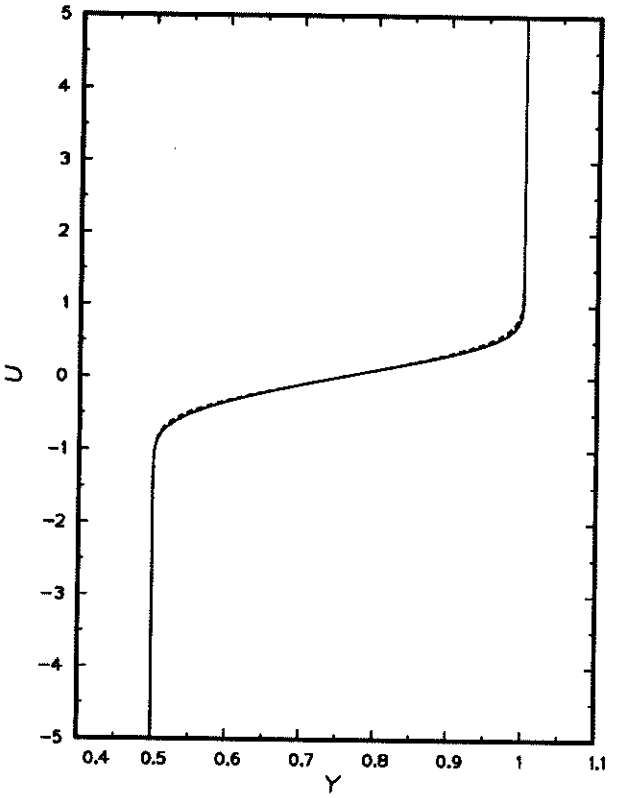

FIGURE 1. Streamwise velocity. $T_{ad}=1$, $M_1=6$ ($M_2=3$), $\bar{T}_2=1$, $H=5$. ——— , without walls (boundary-layer equations); ---- , with walls (full Navier-Stokes equations).

where $\overline{F}(y)$ is the laminar flow quantity and F' is the disturbance.

At the walls, we could apply no-slip boundary conditions. However, the focus of this study is on the shear layer, and the boundary layers are not be important so long as they are much thinner than the shear layer and channel width. Hence we allow fluid slip at the walls but no penetration. Furthermore, heat loss and chemical reaction at the walls are excluded. Boundary conditions for the disturbances at the sidewalls ($z=\pm B/2$) are, therefore,

$$\frac{\partial u'}{\partial z} = \frac{\partial v'}{\partial z} = w' = \frac{\partial \rho'}{\partial z} = \frac{\partial T'}{\partial z} = \frac{\partial p'}{\partial z} = \frac{\partial y'_F}{\partial z} = \frac{\partial y'_O}{\partial z} = 0 \qquad (2)$$

Solutions for the disturbances which satisfy the above boundary conditions are

assumed to have the form:

$$\begin{bmatrix} u' \\ v' \\ w' \\ \rho' \\ T' \\ p' \\ y'_F \\ y'_O \end{bmatrix} = \begin{bmatrix} \hat{u}(y)\cos(2m\pi z/B) \\ \hat{v}(y)\cos(2m\pi z/B) \\ \hat{w}(y)\sin(2m\pi z/B) \\ \hat{\rho}(y)\cos(2m\pi z/B) \\ \hat{T}(y)\cos(2m\pi z/B) \\ \hat{p}(y)\cos(2m\pi z/B) \\ \hat{y}_F(y)\cos(2m\pi z/B) \\ \hat{y}_O(y)\cos(2m\pi z/B) \end{bmatrix} e^{i(\alpha x-\omega t)} \qquad (m=0,1,2,...) \tag{3}$$

where α, m are wavenumbers in the streamwise and spanwise directions, respectively, and ω is the frequency. The perturbation equations are derived by linearizing the compressible Euler equations. Substituting Eq. (3) into the linearized governing equations, we derive a second order ordinary differential equation for the pressure:

$$\hat{p}'' - \left\{ \frac{2\alpha\bar{u}'}{(\alpha\bar{u}-\omega)} + \frac{\bar{\rho}}{\bar{T}}(\alpha\bar{u}-\omega)^2[RXN1] \right\} \hat{p}' -$$

$$\left[\left\{ \alpha^2 + \left(\frac{2m\pi}{B} \right)^2 \right\} - \gamma {M_1}^2 (\alpha\bar{u}-\omega)^2 \left\{ \frac{1}{\bar{T}} + \frac{\bar{\rho}}{\bar{T}}[RXN2] \right\} \right] \hat{p} = 0 \tag{4}$$

where γ is the specific heat ratio and M_1 is the Mach number of the upper stream. $[RXN1]$ and $[RXN2]$ are terms that represent the effect of density variation due to chemical reaction and compressibility on the instability. The boundary conditions at the top and bottom walls become

$$\hat{p}'(H) = \hat{p}'(-H) = 0 \tag{5}$$

With these boundary conditions, Eq. (4) is solved by a combination of the shooting and Newton-Raphson methods.

2.2 Effect of walls

First, the effect of wall on the instability is examined. We begin by looking at the two-dimensional waves (m=0) in the non-reacting flow (T_{ad}=1) with H=5. Because all length scales are nondimensionalized by initial vorticity thickness, H=5 means that wall separation is five times the vorticity thickness, which is small enough to permit interaction between the wall and unstable acoustic modes. Fig. 2 shows the amplification rates and phase speeds as functions of frequency at Mach numbers M_1=0, 2, 3. It shows that when the Mach number of the disturbance relative to either free-stream, is subsonic ($|M_r| < 1$), there is only one unstable mode, and its phase velocity is about the average of two free stream velocities; we can identify this as a Kelvin-Helmholtz mode. The amplification rate of this mode decreases as the Mach number increases, just as in unconfined shear flows. The effect of walls on these modes is weak.

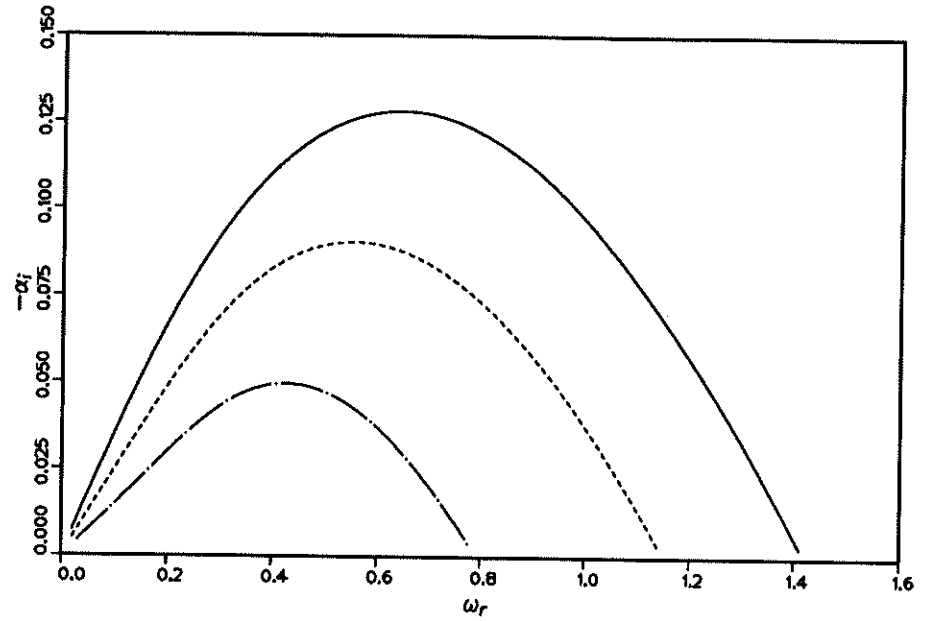

(a)

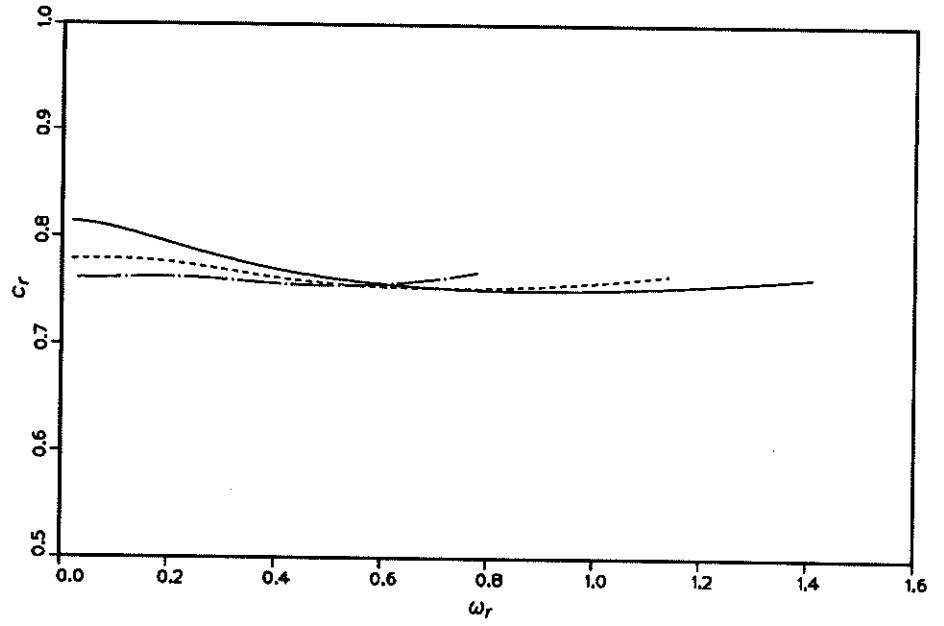

(b)

FIGURE 2. (a) Amplification rates and (b) phase velocities in subsonic relative Mach number. $T_{ad}=1$, $m=0$, $H=5$, $\bar{T}_2=1$. ——— , $M_1=0$; - - - - , $M_1=2$; —·— , $M_1=3$.

When the relative Mach number is supersonic ($|M_r| > 1$), there are many supersonic unstable modes; these are similar to the supersonic modes found by Mack (1984) in boundary layers. These modes arise from reflection of acoustic waves by the walls and do not exist without walls. Fig. 3 shows the growth rates of these unstable modes and the corresponding phase velocities at M_1=6 and M_2=3. There are further unstable modes at higher frequencies; their amplification rates are lower. The unstable modes can be classified into the three families found in unconfined flows, the center, slow, and fast modes. The phase velocities of the fast modes decrease as the frequency increases, while those of slow modes increase with frequency. They all appear to approach the average of the two free-stream velocities. This behavior contrasts with what was found in unconfined flows, in which the phase velocities approach the free-stream velocities. Each mode is unstable only over a relatively narrow frequency band. For this set of parameters, the most unstable mode is a center mode, but it is only slightly more unstable than one of the outer modes.

For the reacting flow with T_{ad}=4 and H=5, the two-dimensional amplification rates and phase velocities at subsonic relative Mach numbers are shown in Fig. 4. Fig. 4a shows the amplification rates of center and slow modes and Fig. 4b shows the amplification rates of fast modes at three different Mach numbers M_1=0, 2, 3. Fig. 4c shows the corresponding phase velocities. The amplification rates of all modes decrease as the Mach number increases. The fast modes have smaller amplification rates than their slow counterparts. When the relative Mach number is supersonic, three families of modes are unstable. Fig. 5 shows the growth rates of these unstable modes and the corresponding phase velocities for M_1=6 and M_2=3. Other unstable modes with lower amplification rates and higher frequencies are not shown. The fast and slow modes have comparable amplification rates, while the center mode is less unstable. Unlike the situation in non-reacting flows, neither phase velocity approaches the average speed. Rather, the phase velocities of the outer modes appear to be almost independent of frequency.

Because the walls change the characteristics of supersonic unstable modes from those found in unconfined flows, the distance between the walls is an important parameter. For two-dimensional modes, m=0, the growth rates are independent of the aspect ratio of the duct, i.e. the breadth has no effect on the stability. We calculated the properties of spatially growing waves at various values of H for fixed upper stream Mach number M_1 and fixed mean velocity and temperature profiles. The instability behavior of the subsonic shear layer hardly varies with the distance between the walls. However, the instability characteristics of supersonic shear layers change considerably as height increases. Fig. 6 shows the maximum amplification rates as functions of H at M_1=6 (M_2=3). The smallest H considered is 5. We consider only the center mode for non-reacting flows (T_{ad}=1) and the slow mode for reacting flows (T_{ad}=4 and 8). The maximum growth rates of both the non-reacting and reacting shear layers increase as the distance between the walls decreases. As expected, reflection of acoustic waves by closely spaced walls prevents radiation of energy and makes the flow more unstable. The effect is much larger in

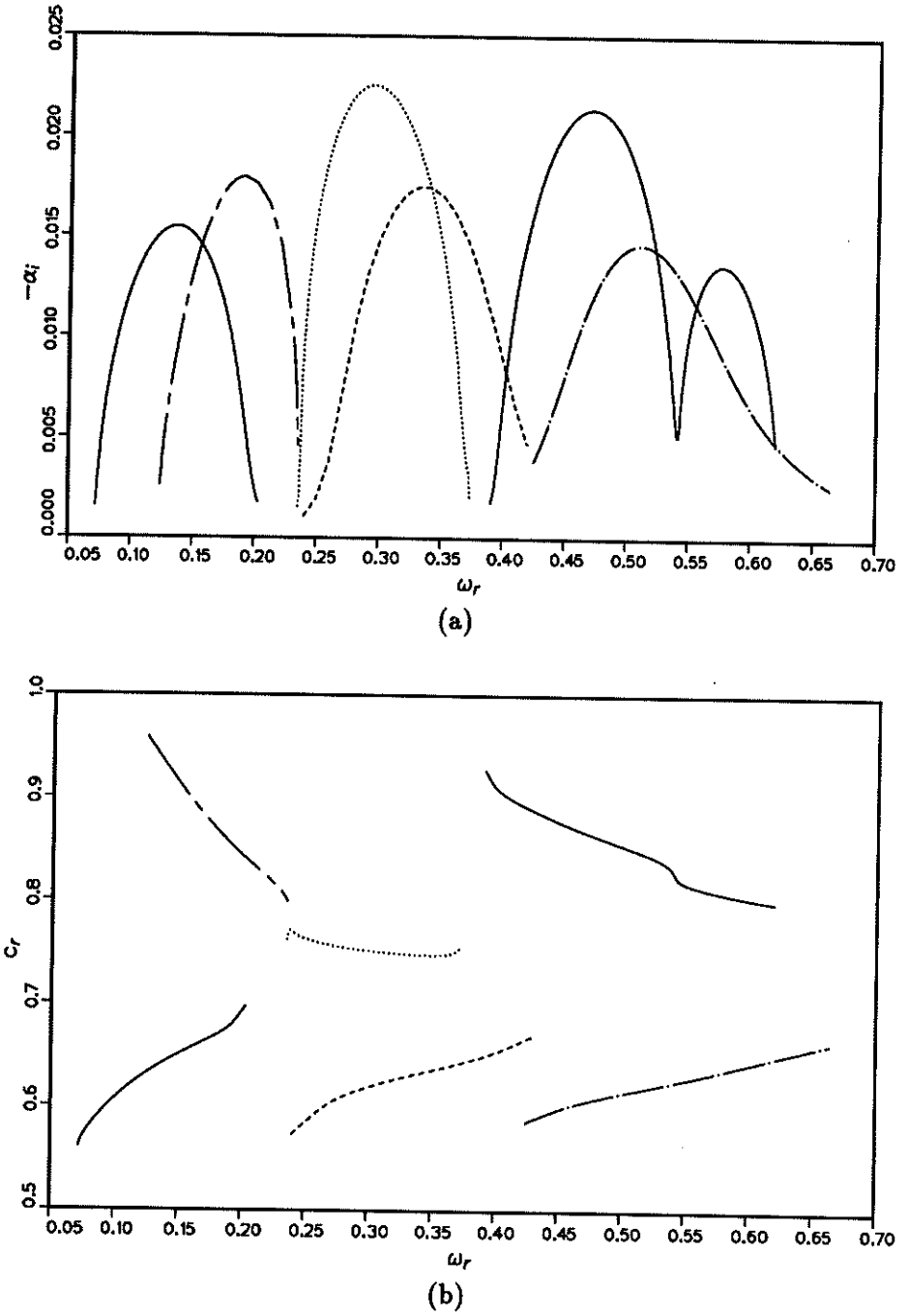

FIGURE 3. (a) Amplification rates and (b) phase velocities in supersonic relative Mach number. $T_{ad}=1$, $M_1=6$, $M_2=3$, $m=0$, $H=5$, $\bar{T}_2=1$.

the non-reacting case for which the maximum growth rate at $H=5$ is about twice as

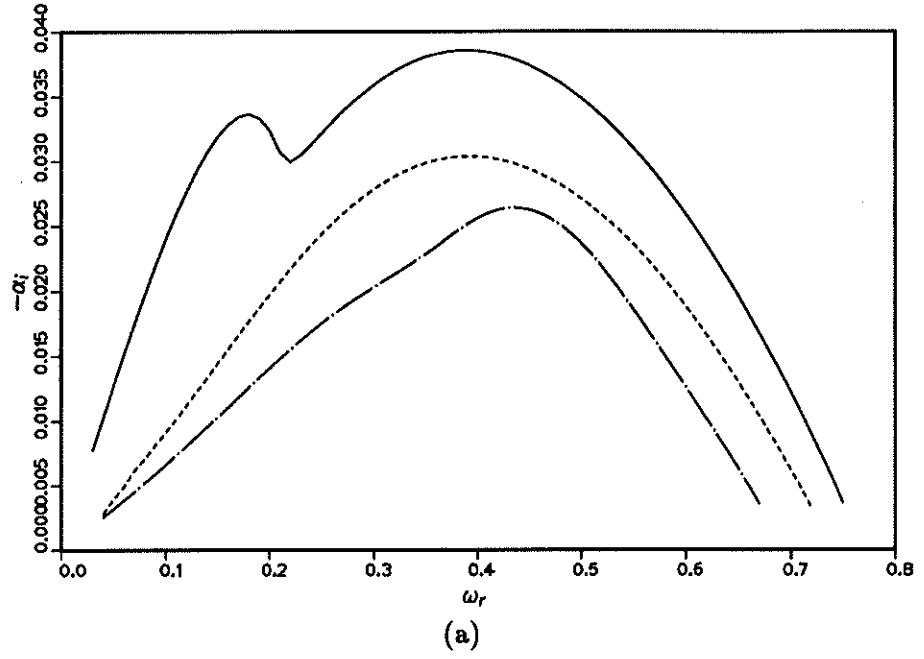

(a)

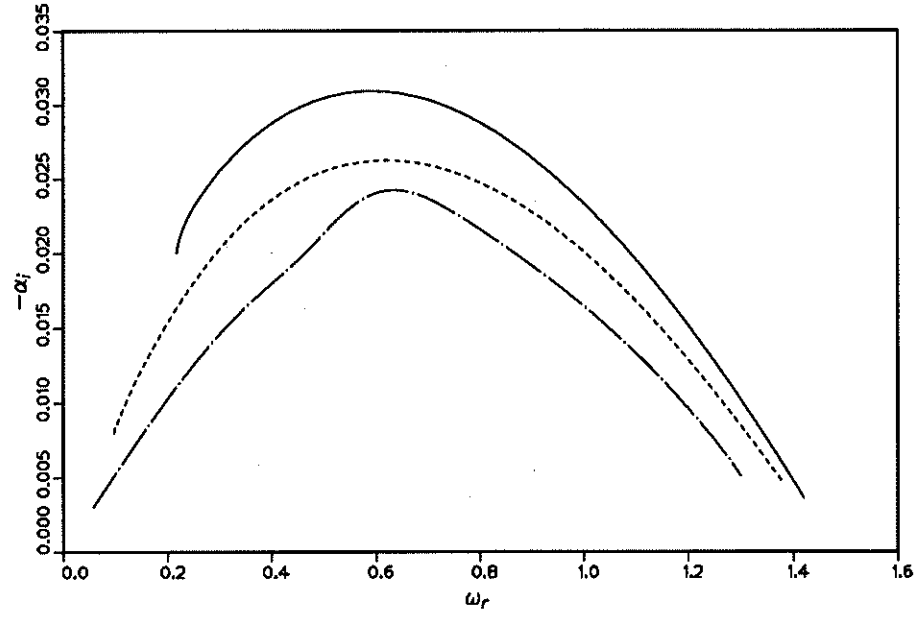

(b)

FIGURE 4. (a) Amplification rates of center and slow modes (b) amplification rates of fast modes in subsonic relative Mach number. $T_{ad}=4$, $m=0$, $H=5$, $\bar{T}_2=1$. ——— , $M_1=0$; - - - - , $M_1=2$; —·— , $M_1=3$.

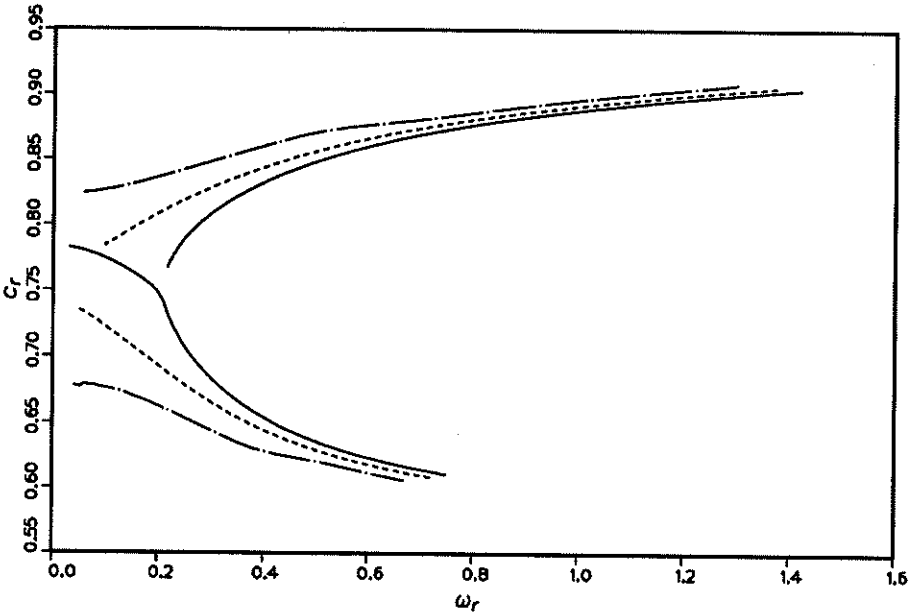

(c)

FIGURE 4. (continued) (c) Corresponding phase velocities in subsonic relative Mach number. T_{ad}=4, m=0, H=5, $\bar{T}_2$=1. ——— , M_1=0; - - - - , M_1=2; —·— , M_1=3.

large as that at H=20. For T_{ad}=4, the maximum growth rate at H=5 is about 1.4 times larger than that at H=20. When H is relatively small ($H < 7.5$), the non-reacting flow (T_{ad}=1) is more unstable than the reacting flow (T_{ad}=4); the reverse is true for large H ($H > 7.5$). For T_{ad}=8, the maximum growth rate increases as H decreases, but the change is small. This flow is more unstable than the cold flow (T_{ad}=1) and moderate heat release flow (T_{ad}=4) at all H considered here.

2.3 Three-dimensional modes

In partially confined-channel flows, which have no sidewalls, the disturbances are of the travelling-wave form in the transverse direction (Shin and Ferziger 1991). The only difference between partially-confined flows and rectangular-channel flows is the boundary condition at the side walls, Eq. (1). We studied the growth rate of three-dimensional modes in both types of flows. Because heat release favors the two-dimensional instability, we considered only the non-reacting case (T_{ad}=1); because walls have little effect on the low-speed flow, only high-speed flows (M_1=6, M_2=3) were studied. Fig. 7 shows the amplification rates of the most amplified modes at several angles for the case without sidewalls. The growth rates of three-dimensional modes (θ=70°) are higher than those of two-dimensional modes (θ=0°). This result shows the behavior similar to that of free shear layers (Shin & Ferziger 1991). Thus the top and bottom walls favor three-dimensional instabilities when there are no sidewalls.

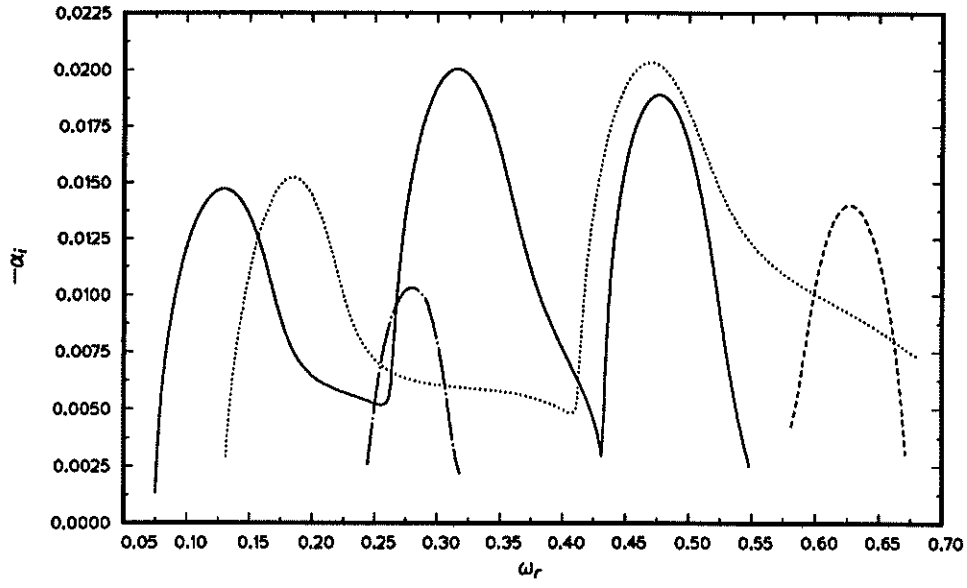

(a)

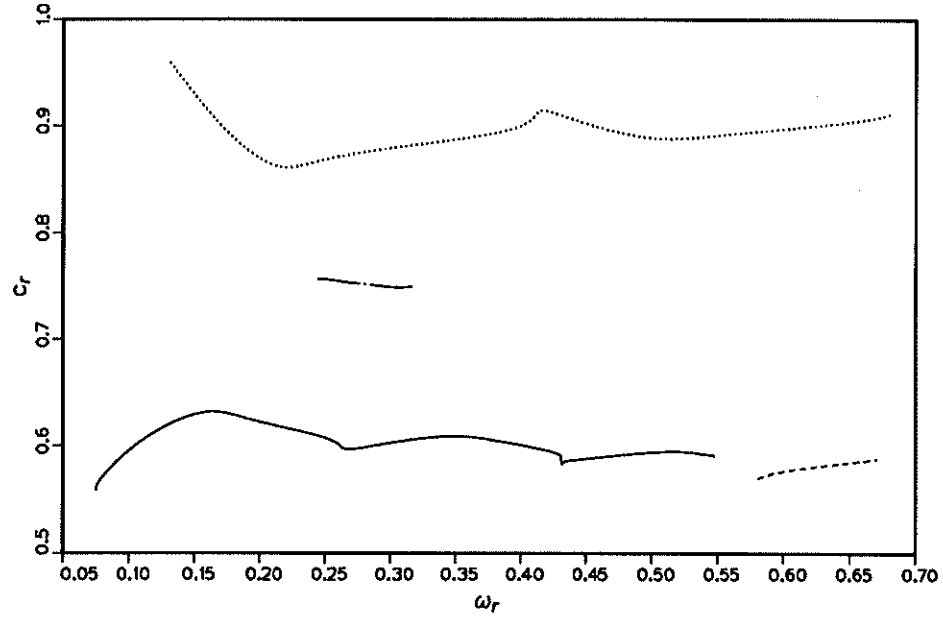

(b)

FIGURE 5. (a) Amplification rates and (b) phase velocities in supersonic relative Mach number. T_{ad}=4, M_1=6, M_2=3, m=0, H=5, $\bar{T}_2$=1.

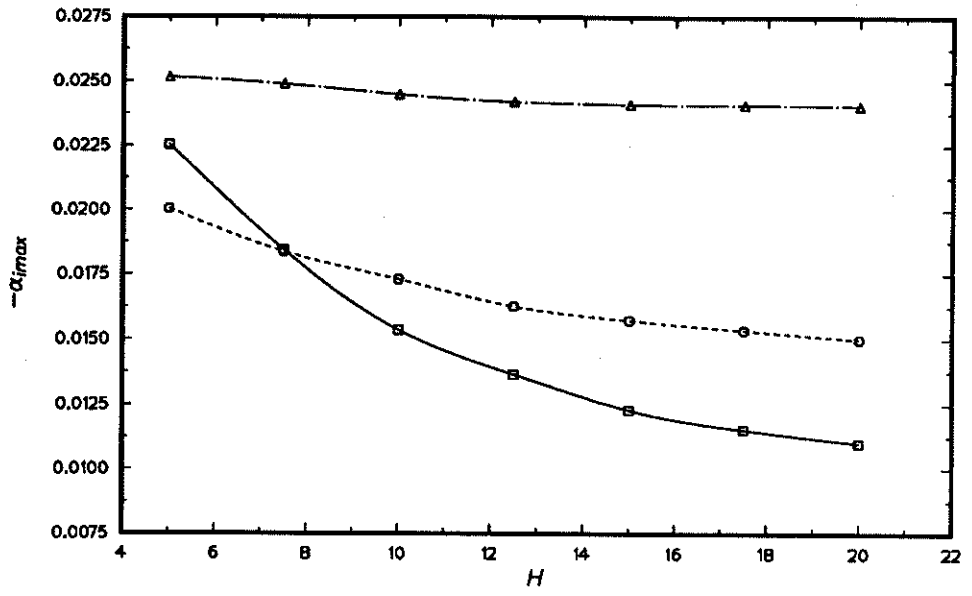

FIGURE 6. Maximum amplification rates versus H. m=0, M_1=6, M_2=3, $\bar{T}_2$=1. □, T_{ad}=1, center mode; ○, T_{ad}=4, slow mode; △, T_{ad}=8, slow mode.

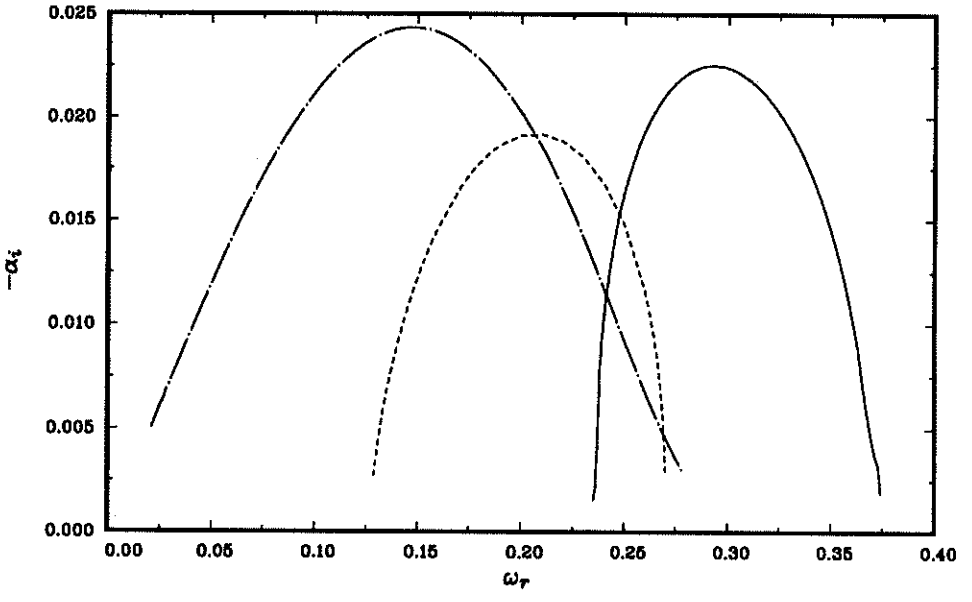

FIGURE 7. Amplification rates in partially confined flow at T_{ad}=1. H=5, $\bar{T}_2$=1, M_1=6, M_2=3. ——, θ=0°; - - - -, θ=30°; —·—, θ=75°.

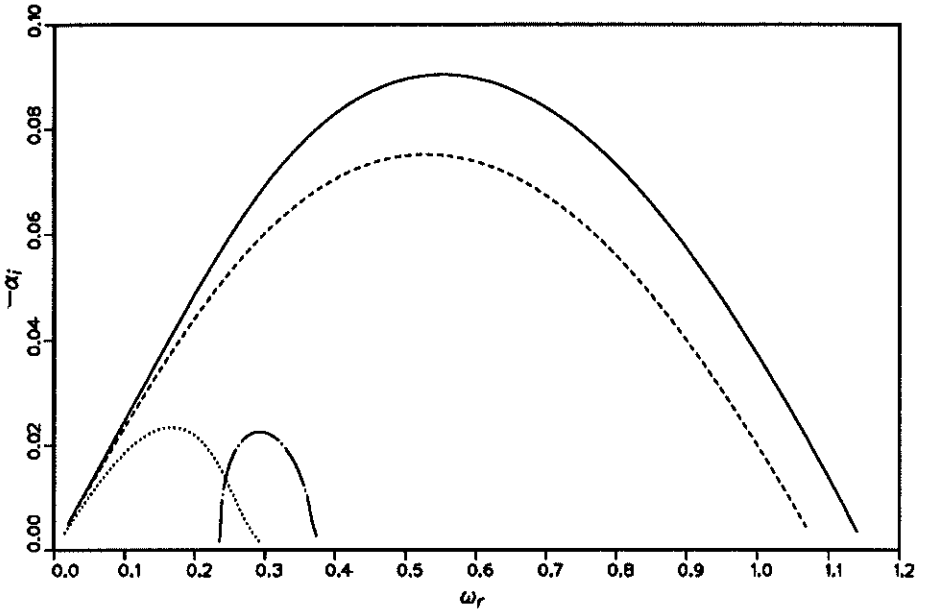

(a)

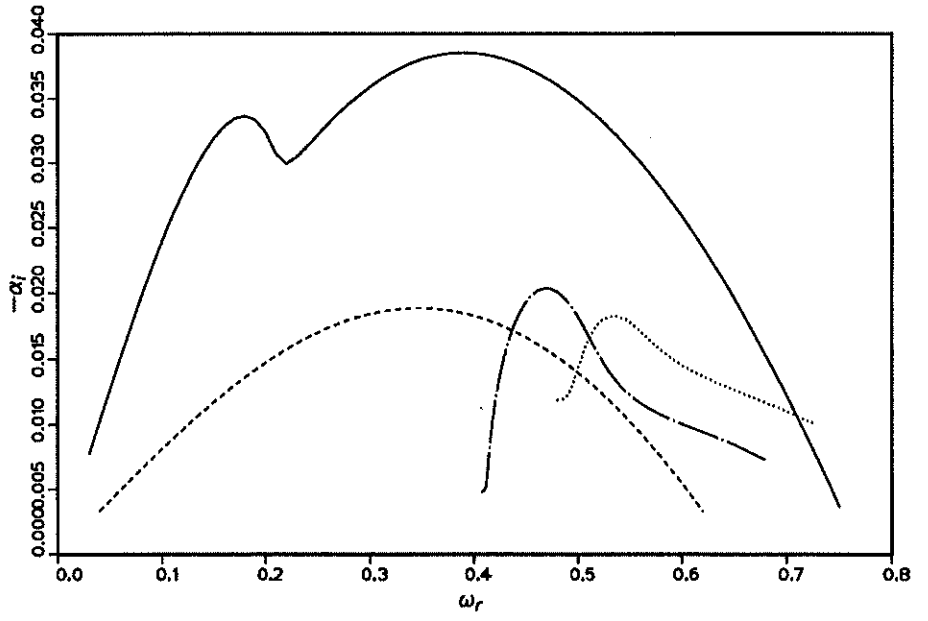

(b)

FIGURE 8. Amplification rates in rectangular channel flow for (a) non-reacting (T_{ad}=1) and (b) reacting (T_{ad}=4) flows. $B/2=H=5$, $\bar{T}_2=1$. ——— , $M_1=2$, $m=0$; - - - - , $M_1=2$, $m=1$; —·— , $M_1=6$, $m=0$; ····· , $M_1=6$, $m=1$.

A rectangular channel might display three-dimensional instabilities due to reflections from the sidewalls. The transverse-boundary conditions (Eq. (1)) will allow only integer values of the transverse wavenumber m. We investigated the three-dimensional instability modes for both non-reacting (T_{ad}=1) and reacting (T_{ad}=4) rectangular-channel flows. We chose 10 as the wall height. The breadth of the channel B was 10 in this study. We studies two different Mach numbers, M_1=2 and 6 (M_2=1 and 3); the first is considered as a low-speed flow and the second, a high-speed flow.

Fig. 8a shows the amplification rates for the non-reacting cases. We consider only the center mode for non-reacting flows (T_{ad}=1) and the slow mode for reacting flows (T_{ad}=4) because they are the most unstable modes for the respective flows; m=0 corresponds to two-dimensional modes and m=1 to three-dimensional modes. We found only damped modes for $m > 1$. In the low-speed flow (M_1=2), the three-dimensional mode (m=1), for which the propagation angle of the most amplified mode is 42°, has lower amplification rates than the two-dimensional mode (m=0); this is similar to what we found for unconfined flows. In high-speed flow (M_1=6), the three-dimensional mode (m=1) has lower amplification rates and the propagation angle of the most amplified three-dimensional mode is 70°. This result shows that three-dimensional modes have lower amplification rates than two-dimensional modes in high-speed non-reacting flows unlike unconfined flows. Thus side walls favor two-dimensionality.

Fig. 8b shows the results for the reacting cases. For the three-dimensional modes, the propagation angle of the most unstable mode is 48° at low-speed (M_1=2) and 46° at high-speed (M_1=6), respectively. However, the most amplified modes are still two-dimensional (m=0), which is similar to the situation in unconfined reacting shear layers. As a consequence, we consider only two-dimensional modes below.

2.4 Effect of Mach number and heat release

This section studies the effect of the Mach number and heat release on the maximum growth rates of instabilities in confined shear layers. The wall height is fixed at 10. Fig. 9 gives the maximum amplification rate versus the upper-stream Mach number and indicates that the maximum growth rate of the most unstable two-dimensional mode decreases with Mach number in both non-reacting (T_{ad}=1) and reacting (T_{ad}=4) flows. They appear to approach asymptotic values for $M_1 > 4$ or $M_c > 1$, where M_c is the isentropic convective Mach number defined by Papamoschou and Roshko (1988).

In the non-reacting case, there is little difference between the unconfined and the confined flows when the isentropic convective Mach number is subsonic ($M_1 < 4$). When the isentropic convective Mach number is supersonic ($M_1 > 4$), the reflection of acoustic waves by the walls makes the confined flow more unstable than the unconfined flow. At M_1=8, the maximum growth rate of the confined flow is about four times larger than that of the unconfined flow. However, it is small (about 16%) compared to the growth rate of the cold flow at M_1=0. The reacting flow shows a similar qualitative trend. Heat release seems to reduce the compressibility effect even more in confined flows; the ratio of the maximum amplification at M_1=8 to

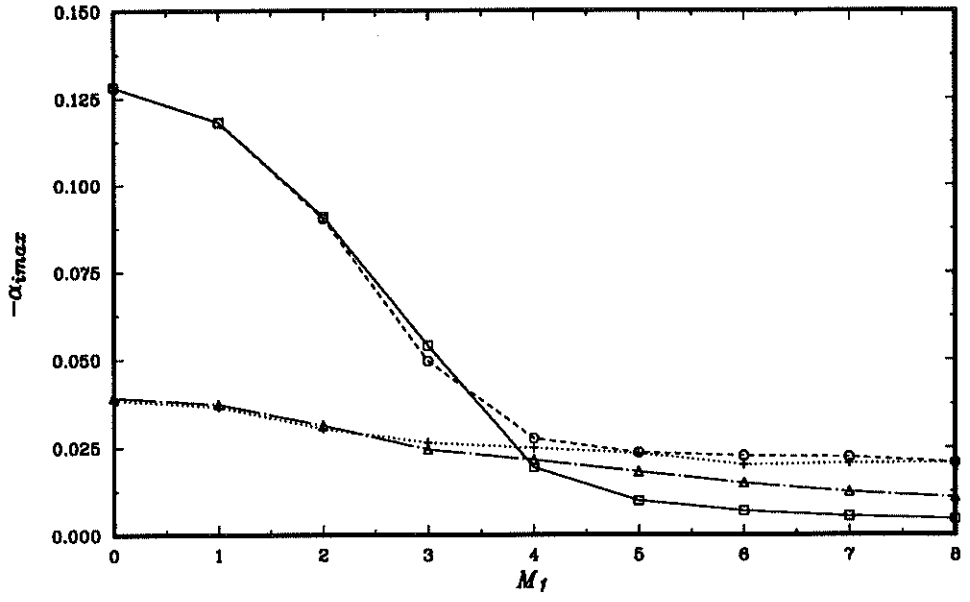

FIGURE 9. Maximum amplification rates versus M_1. m=0, H=5, $\bar{T}_2$=1. □ , T_{ad}=1, unconfined; ○ , T_{ad}=1, confined; △ , T_{ad}=4, unconfined; +, T_{ad}=4, confined.

that at M_1=0 is about two, which is half of the ratio in the non-reacting flow.

Fig. 10 shows the effect of heat release on the maximum amplification rate of unstable modes for low-speed (M_1=1) and high-speed (M_1=6) flows. In the low-speed flow, the walls make little difference. Heat release stabilizes the low-speed flow; the maximum amplification rate for T_{ad}=8 is about 15% of the cold flow value. At M_1=6, the confined flows are more unstable than the unconfined flows. When H=5, heat release slightly stabilizes the flow for $T_{ad} < 4$ but destabilizes for $T_{ad} > 4$ (see Fig. 6). As the distance between the walls increases, the difference between the confined and unconfined flow behavior becomes small. For H=20, the maximum amplification rate increases as heat release increases, which is what happens in the unconfined flow. The change of the maximum growth rate with the Mach number is large in cold flow (T_{ad}=1); it becomes smaller as the heat release increases. The effect of the walls on the growth rate becomes negligible at large heat release. At high Mach numbers, the amplification rates change less with T_{ad} than at low Mach numbers; this is consistent with the behavior of the supersonic-ramjet combustors (Drummond 1991, private communication).

2.5 Eigenfunctions

This section studies contours of the flow variables derived from the most unstable two-dimensional eigenfunctions and the mean flow. The eigenfunctions are normalized so that the maximum absolute value of $\hat{u}$ is unity. We chose H=5 in order to include the effect of confinement. We considered only the center and slow modes; the fast mode can be obtained by reflection of the slow mode.

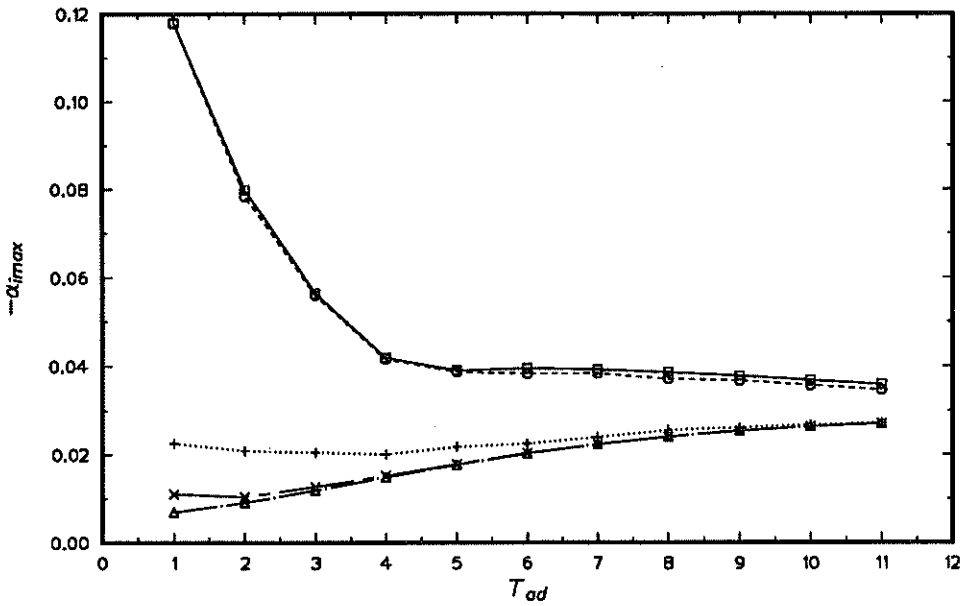

FIGURE 10. Maximum amplification rates versus T_{ad}. m=0, $\bar{T}_2$=1. □ , M_1=1, unconfined; ○ , M_1=1, confined, H=5; △ , M_1=6, unconfined; +, M_1=6, confined, H=5; ×, M_1=6, confined, H=20.

Fig. 11 shows the contours of various quantities produced by the supersonic center mode for the non-reacting (T_{ad}=1) flow at M_1=6 (M_2=3). The contours of vorticity in Fig. 11a are qualitatively different from those for the corresponding low-speed mode. The two elementary clockwise vortices of the low-speed cold flow have been replaced by a single vortex in the center of the layer. The pressure contours in Fig. 11b show clearly the radiative nature of the supersonic center mode. Unlike the outer modes that radiate only to one free stream, the center modes are supersonic relative to the both streams, and the associated compression (solid line) and expansion waves (dashed line) propagate toward both boundaries. The patterns of compression/expansion waves in Fig. 11b suggest that the waves are reflected by the walls. The reflections carry energy back to the shear layer, producing feedback that makes confined shear layers more unstable than free shear layers. Mack reported a similar observation for boundary layers (1984).

From the pressure contours, we measured the Mach angle μ and estimated the convective Mach number M_c based on the most unstable mode (Mack 1975, Zhuang *et al.* 1990) from

$$M_c = \frac{1}{\sin\mu} \tag{6}$$

Measurement of the Mach angle from Fig. 11b gives about μ=40°, from which we estimate the convective Mach number to be approximately 1.55. The convective Mach number based on the phase velocity of the most unstable mode is 1.49; this agreement is considered to be very good.

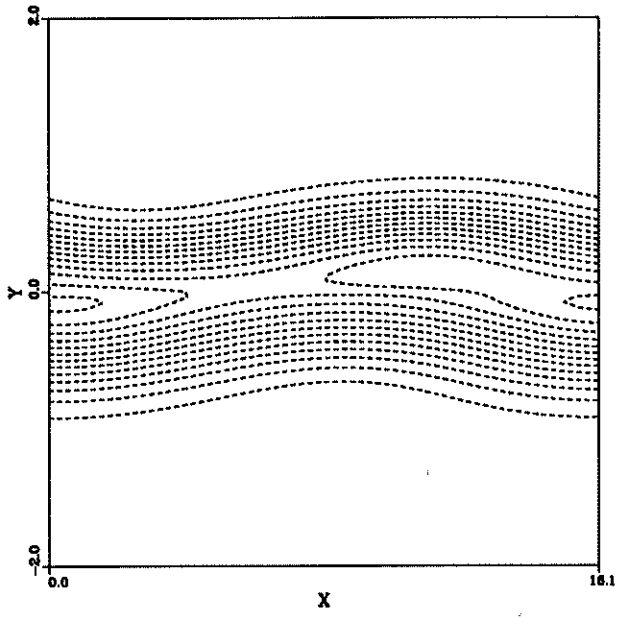

(a) max=0., min=-0.266

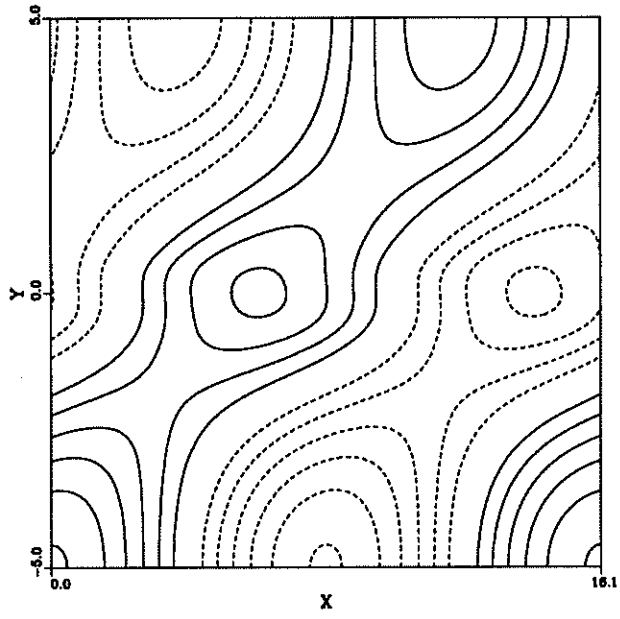

(b) max=1.122, min=0.878

FIGURE 11. Contour plots from linear eigenfunctions of the non-reacting confined flow (center mode). (a) vorticity (b) pressure. M_1=6 (M_2=3), $\bar{T}_2$=1, T_{ad}=1, m=0, H=5.

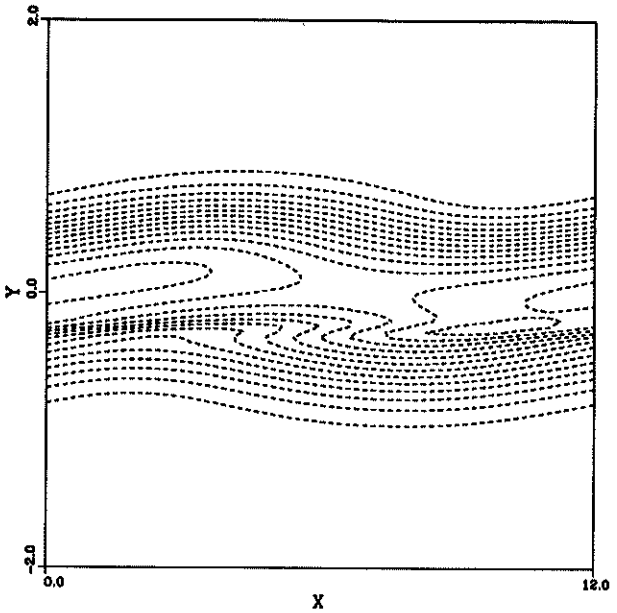

(a) max=0.001, min=-0.270

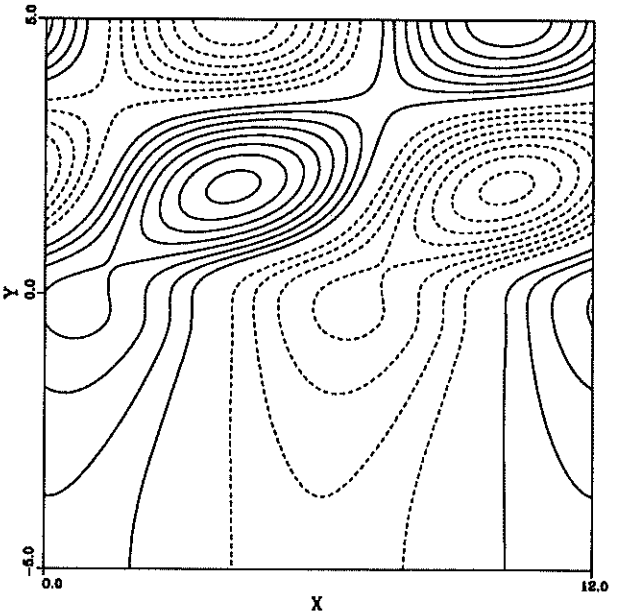

(b) max=1.167, min=0.833

FIGURE 12. Contour plots from linear eigenfunctions of the non-reacting confined flow (slow mode). (a) vorticity (b) pressure. M_1=6 (M_2=3), $\bar{T}_2$=1, T_{ad}=1, m=0, H=5.

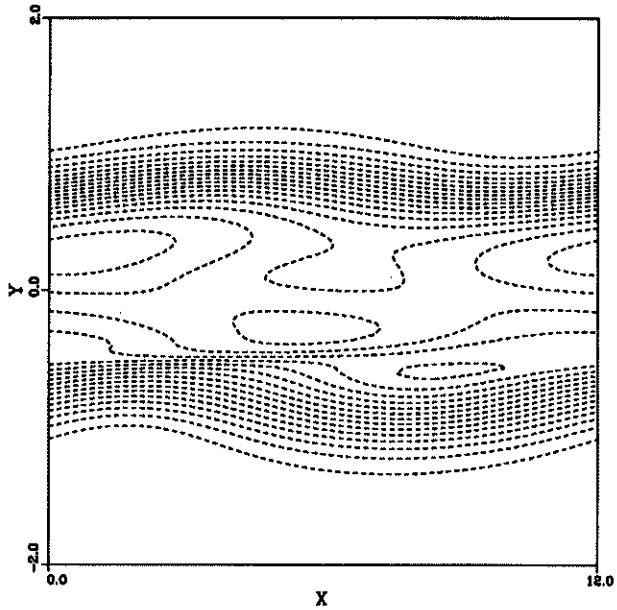

(a) max=0.003, min=-0.175

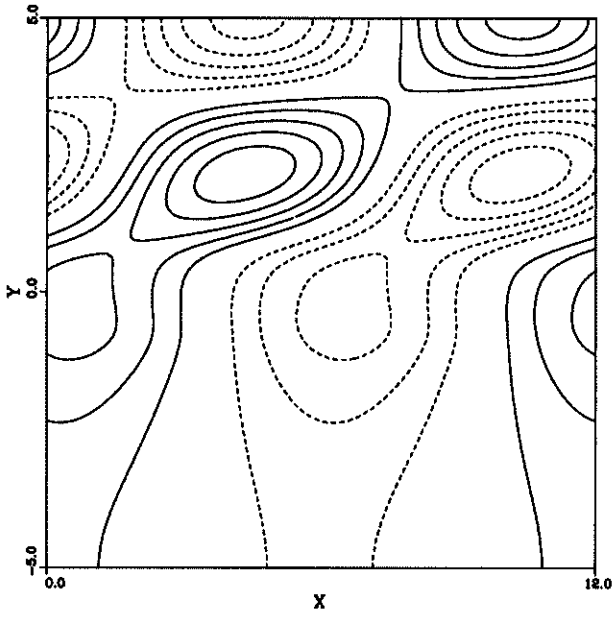

(b) max=1.116, min=0.884

FIGURE 13. Contour plots from linear eigenfunctions of the reacting confined flow (slow mode). (a) vorticity (b) pressure. M_1=6 (M_2=3), $\bar{T}_2$=1, T_{ad}=4, m=0, H=5.

Figs. 12-13 show contours for non-reacting and reacting supersonic slow modes at

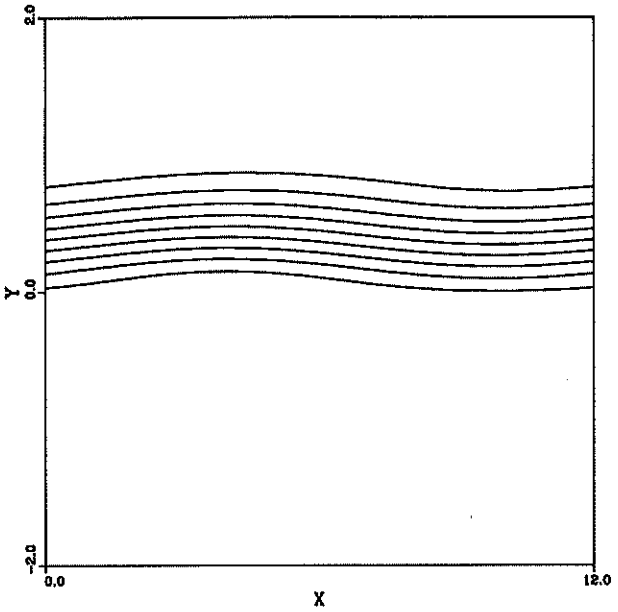

(c) max=1.0, min=0.0

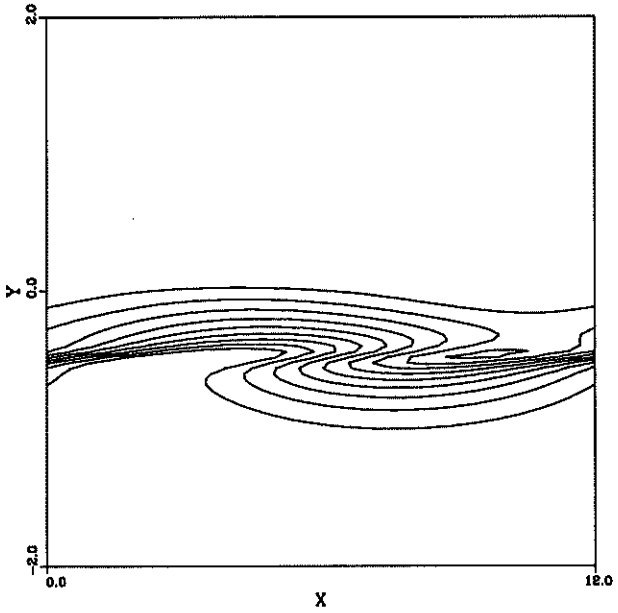

(d) max=1.0, min=0.0

FIGURE 13. (continued) Contour plots from linear eigenfunctions of the reacting confined flow (slow mode). (c) fuel (d) oxidizer. M_1=6 (M_2=3), $\bar{T}_2$=1, T_{ad}=4, m=0, H=5.

M_1=6 (M_2=3). The patterns are similar to those for the corresponding unconfined flows except for the pressure contours. The latter again show reflections of compression/expansion waves propagating at Mach angle μ=27° for the non-reacting flow and μ=26° for the reacting flow. The convective Mach numbers according to Eq. (6) are 2.20 for the non-reacting flow and 2.28 for the reacting flow, while the convective Mach numbers based on the corresponding most unstable modes are 2.22 and 2.33 respectively; the agreement is again very good. The contours of the reactant concentrations in Figs. 13c-d show that the slow mode principally affects the oxidizer because the oxidizer occupies the lower part of the layer. The fuel distribution is hardly perturbed, so the supersonic slow mode will not yield much mixing between reactants in confined reacting flows.

2.5 Streaklines

A streakline is a line connecting the current positions of the fluid particles that have passed through the same point. Smoke or dye injectors allow one to visualize streaklines experimentally. In this subsection, we calculate streaklines from the linear stability eigenfunctions. The velocity components of the disturbed shear layer, u and v, will have the form

$$u = \bar{u}(y) + a\Re[\hat{u}(y)e^{i(\alpha x-\omega t)}], \qquad v = a\Re[\hat{v}(y)e^{i(\alpha x-\omega t)}] \tag{7}$$

The position of a particle at time t, $(x(t), y(t))$, can be calculated from

$$\frac{dx}{dt} = u(x(t), y(t), t), \qquad \frac{dy}{dt} = v(x(t), y(t), t) \tag{8}$$

We calculate a pathline with the initial conditions

$$x(t_0) = x_0, \qquad y(t_0) = y_0 \tag{9}$$

In our calculation, we chose a=0.0005 and t=0 and considered the most unstable two-dimensional modes. Streaklines for confined flows at high Mach numbers M_1=6 (M_2=3) are given in Fig. 14 for both cold (T_{ad}=1) and reacting (T_{ad}=4) flows. Only the center and slow modes are shown; the fast mode can be obtained by reflection of the slow mode. In contrast to the behavior of the low-speed cold flow, the streaklines of the non-reacting center mode in high Mach number confined shear flows do not indicate roll-up, which suggests that the coherent structures might not be produced and that mixing between the fuel and oxidizer will not be active. As in unconfined flows, the slow mode primarily disturbs the lower part of the mixing layer, leaving the upper part mostly undisturbed. The reverse is true for the fast mode. Thus the outer modes in confined supersonic mixing layers do not cause roll-up, and mixing between the fuel and oxidizer will not be strong.

3. Summary

In this work, we considered the inviscid stability of the confined compressible reacting mixing layer using laminar-flow profiles generated from solutions of the

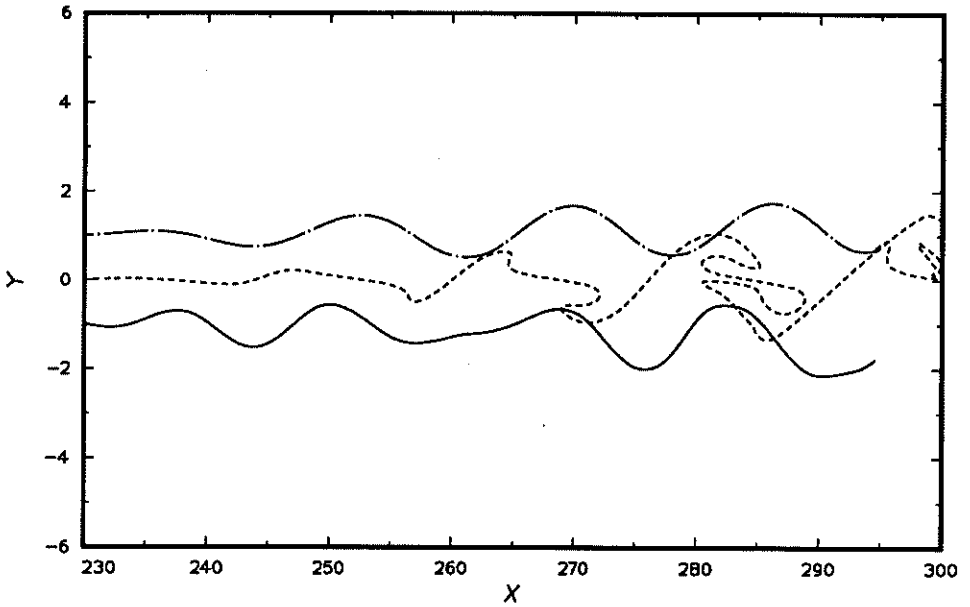

(a)

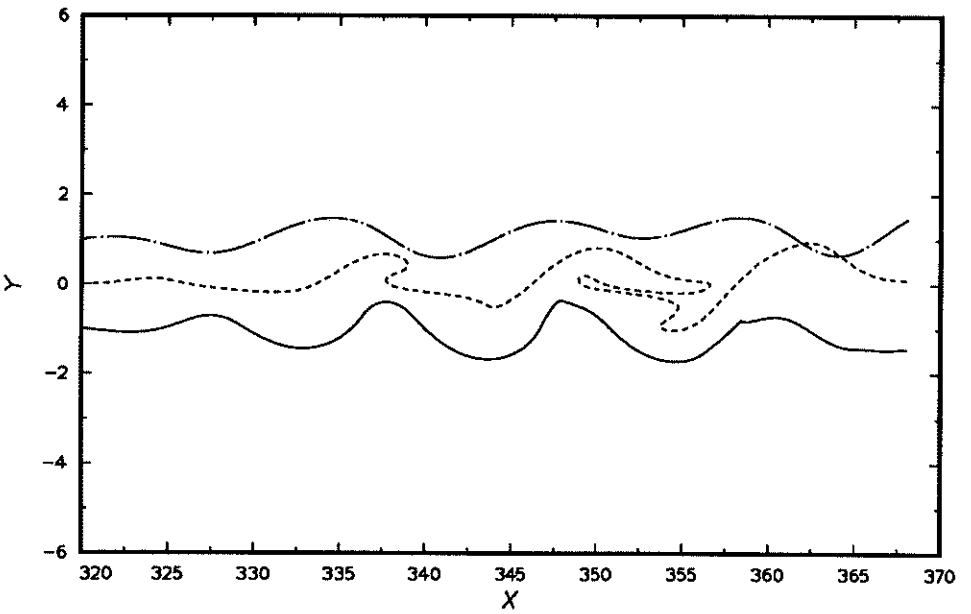

(b)

FIGURE 14. Streaklines for the confined shear layers at M_1=6 (M_2=3). (a) non-reacting center mode (T_{ad}=1) (b) non-reacting slow mode (T_{ad}=1). $\bar{T}_2$=1, m=0, H=5.

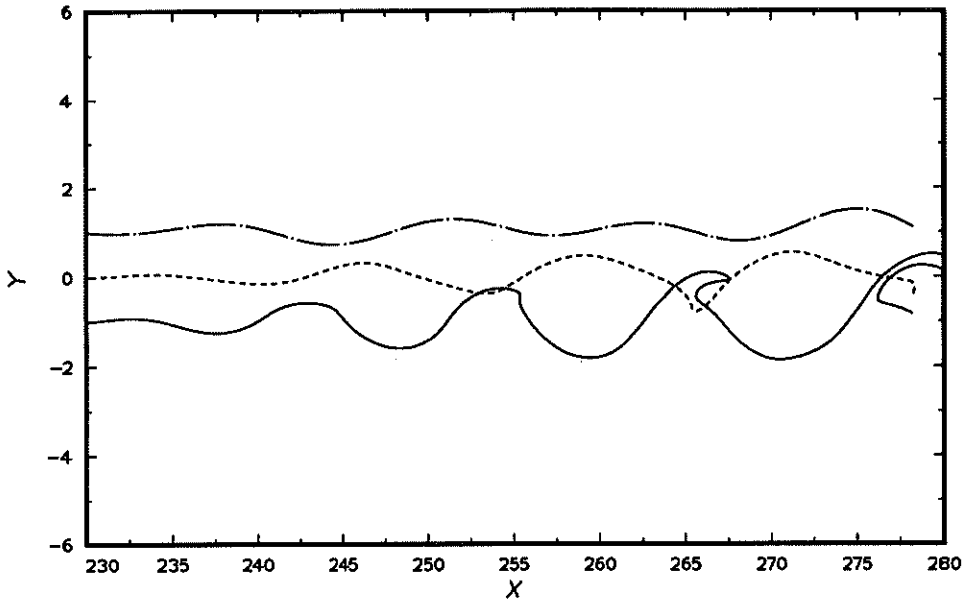

(c)

FIGURE 14. (continued) Streaklines for the confined shear layers at M_1=6 (M_2=3). (c) reacting slow mode (T_{ad}=4). $\bar{T}_2$=1, m=0, H=5.

compressible boundary-layer equations with finite rate chemistry. We found that reflection of supersonic disturbances by the walls makes the mixing layer more unstable than the unconfined free shear layer. Decreasing the distance between the walls makes the flow more unstable. Subsonic disturbances are relatively unaffected by the walls. The most unstable supersonic disturbances are two-dimensional in both the partially confined and rectangular channel flows. Heat release and Mach number hardly change the maximum growth rates of supersonic disturbances. The growth rate of the supersonic mixing layer is very small compared to the corresponding incompressible mixing layer value. The supersonic center mode radiates into both boundaries, whereas the outer modes propagate only to one boundary with respect to which they are supersonic. Pressure contours show the reflection of compression/expansion waves that propagate at the Mach angle. The reactants are not strongly mixed by supersonic instabilities because they disturb mainly one side of the layer.

REFERENCES

GREENOUGH, J., RILEY, J., SOESTRISNO, M & EBERHARDT, D. 1989 The effect of walls on a compressible mixing layer. *AIAA 89-0372.*

MACK, L. M. 1975 Linear Stability and the Problem of Supersonic Boundary-Layer Transition. *AIAA Journal.* **13,** 278-289.

MACK, L. M. 1984 Boundary-Layer Linear Stability Theory. *Special Course on Stability and Transition of Laminar Flow, AGARD Report.* **709**, 3-1 to 3-81.

MORRIS, P. J. & GIRIDHARAN, M. G. 1991 The effect of walls on instability waves in supersonic shear layers. *Phy. of Fluids.* **3**, 356–358.

PAPAMOSCHOU, D. & ROSHKO, A. 1988 The compressible turbulent shear layer: an experimental study. *J. Fluid Mech.* **197**, 453–477.

SHIN, D. S. & FERZIGER, J. H. 1991 Stability of compressible reacting mixing layer. *AIAA 91-0372.*

TAM, K. W. & HU, FANG Q. 1989 The instability and acoustic wave modes of supersonic mixing layers inside a rectangular channel. *J. Fluid Mech.* **203**, 51–76.

ZHUANG, M., DIMOTAKIS, P. E. & KUBOTA, T. 1990 The effect of walls on a spatially growing supersonic shear layer. *Phy. of Fluids.* **2**, 599–604.